APPLICATION OF THE METHOD OF AUXILIARY SOURCES (MAS) TO THE ANALYSIS OF ELECTROMAGNETIC SCATTERING FROM DIELECTRIC SURFACES WITH CURVED WEDGES

Vissarion G. Iatropoulos, Minodora-Tatiani Anastasiadou, Hristos T. Anastassiu

Department of Informatics Engineering
Technological Educational Institute (TEI) of Central Macedonia,
End of Magnisias Str., GR-62124 Serres,
GREECE
hristosa@teiser.gr

Tel.: +30 23210 49376
Fax: +30 23210 49128

Abstract

The Method of Auxiliary Sources (MAS) is applied to Transverse Magnetic (TM) plane wave scattering from infinite, dielectric, non-smooth cylinders. The geometry of the scatterer is assumed to include curved wedges, defined as intersections of circular arcs, for the first time in literature. The auxiliary surface is shaped in various patterns, to study the effect of its form on the MAS accuracy. In addition to the standard, conformal shape, several deformations are tested, where the auxiliary sources are allowed to approach the tip of the wedge. It is demonstrated that such a procedure leads to significant improvement of the numerical results accuracy. Comparisons of schemes are presented, and the optimal auxiliary source location is proposed.

1. INTRODUCTION

The Method of Auxiliary Sources (MAS) [1] is a numerical technique that has successfully been invoked in computational electromagnetics, in a wide range of radiation and scattering phenomena [2]. MAS is somewhat similar to the Point Matching version of the Method of Moments (MoM), however the auxiliary current sources are not located on the surface boundaries, but inside the radiator/scatterer. The method has been shown to be mathematically rigorous, since the basis functions set used in the field expansions has been proven to be complete [3], which is not always easy to prove in MoM. Moreover, unlike MoM, MAS does not face singularity problems, it avoids time-consuming numerical integration at every stage of the solution, and its algorithmic implementation is much more straightforward.

Although MAS has been utilized in several problems with various geometries and materials, further research is necessary to determine the optimal source location for arbitrary configurations. Particular complications arise when the outer boundary of the scatterer contains wedges, i.e. when the analytical expression of the boundary is not differentiable. In that case, it has been observed that the solution accuracy is depleted, because the boundary condition close to the wedge tip is hard to satisfy adequately. To apply MAS to such configurations, a set of auxiliary sources (AS's) is situated on a fictitious surface, which is generally conformal to the actual boundary, except in the neighborhood of the tips. In the areas surrounding the wedges, the AS's are densely packed and located very close to the tips, to account for the edge effects, as suggested in [4]. Similar strategies were employed in the case of a scattering problem associated with coated Perfectly Electric Conducting (PEC) surfaces including wedges [5], where the surface was modeled via the Standard Impedance Boundary Condition (SIBC) [6].

Although this deformation of the auxiliary surface has proven efficient for straight wedges, in particular forming right angles, no evidence is known from the literature about its applicability to arbitrarily shaped wedges. The aim of this paper is to investigate whether MAS accuracy is enhanced through this deformation, when the wedge is shaped as an intersection of circular arcs with non-coincident centers. The scatterer is thus defined as a dielectric, infinite cylinder, with eye-shaped cross-section. The auxiliary surface is generally maintained as conformal to the scattered boundary, except in the neighborhood of the wedge tips, where various deformation schemes are employed, and accuracy comparisons are drawn.

The format of the paper is as follows: Section 2 quickly recapitulates the mathematical formulation of MAS for dielectric scatterers, illuminated by a transverse magnetic (TM) polarized plane wave. Section 3 proposes several algorithms for the deformation of the auxiliary surfaces close to the wedge tips. Section 4 includes several numerical results for the eye-shaped scatterer and checks the satisfaction of the boundary condition. Finally, section 5 summarizes the method and draws useful conclusions.

A $+j\omega t$ behavior is assumed and suppressed throughout the paper.

2. MAS FOR EYE-SHAPED DIELECTRIC SCATTERERS

We assume a dielectric, infinitely long cylinder with cross section that resembles an eye (Fig. 1a). The dielectric is assumed to be linear, homogeneous and isotropic. The geometry of the scatterer, depicted in blue, comprises two circular arcs with identical radii equal to ρ, but with different centers. In particular, the Cartesian coordinates of the upper arc are given by

$$x_u = \rho cos\varphi,\ y_u = \rho sin\varphi - d \qquad (1)$$

whereas those of the lower arc are given by

$$x_l = \rho cos\varphi,\ y_l = \rho sin\varphi + d \qquad (2)$$

where φ is the azimuth angle and $\pm d$ is the vertical displacement of each arc center, taken equal to the arc apothem (see Fig. 1b). Obviously, φ does not range in the entire $[0,2\pi)$ interval, but is limited by the arc width itself, given by $\varphi_{arc} = 2\arccos\frac{d}{\rho}$. The scatterer is illuminated by a TM plane wave impinging from azimuth angle equal to φ_{inc}. Therefore the incident electric field $\boldsymbol{E}_{inc}$ is given by

$$\boldsymbol{E}_{inc}(x,y) = E_0 \exp\{jk_0(xcos\varphi_{inc} + ysin\varphi inc\boldsymbol{z} \qquad (3)$$

where E_0 is the amplitude of the incident electric field and k_0 is the free space wavenumber. The incident magnetic field $\boldsymbol{H}_{inc}$ is given by

$$\boldsymbol{H}_{inc}(x,y) = -\frac{E_0}{\zeta_0}(\sin\varphi_{inc}\hat{\boldsymbol{x}} - \cos\varphi_{inc}\hat{\boldsymbol{y}}) \exp\{jk_0(xcos\varphi_{inc} + ysin\varphi_{inc})\} \qquad (4)$$

where ζ_0 is the free space intrinsic impedance. To solve the scattering problem via MAS, two sets of AS's are defined, each one of multitude N, as shown in Fig. 1a. In standard MAS formulation both inner and outer auxiliary surfaces are conformal to the scatterer boundary. The electric field due to the n^{th} inner AS, located at point $\boldsymbol{r}_n$ and radiating in the outer space is

$$E_{sn}(\boldsymbol{r}) = \hat{\boldsymbol{z}}E_n H_0^{(2)}(k_0|\boldsymbol{r} - \boldsymbol{r}_n|) \qquad (5)$$

where E_n is the corresponding unknown weight, $(n = 1,2,\dots,N)$, and $H_0^{(2)}$ is the Hankel function of zero order and second kind. The corresponding magnetic field of the n^{th} auxiliary source is obviously proportional to the curl of (5), given explicitly in [5]. Similar expressions hold for the outer AS's, radiating in the inner space of the scatterer, except for k_0 and ζ_0, which have to be replaced by k and ζ respectively, corresponding to the scatterer's dielectric properties. The total scattered E field is expressed as superposition of the fields in (5) and the H field accordingly. By applying the boundary conditions for both fields at N collocation points (CP's) (x_m, y_m) $(m = 1,2,\dots,N)$ of the scattering boundary (blue dots in Fig. 1a), we cast a linear system of equations

$$[\boldsymbol{Z}]\{\boldsymbol{I}\} = \{\boldsymbol{V}\} \qquad (6)$$

where $\{\boldsymbol{I}\}$ is the column vector of the unknown weights E_n, $[\boldsymbol{Z}]$ is a square matrix of size $2N \times 2N$ with elements determined by the interaction between AS's and CP's and $\{\boldsymbol{V}\}$ is the column vector of the incident E and H fields calculated at the CP's.

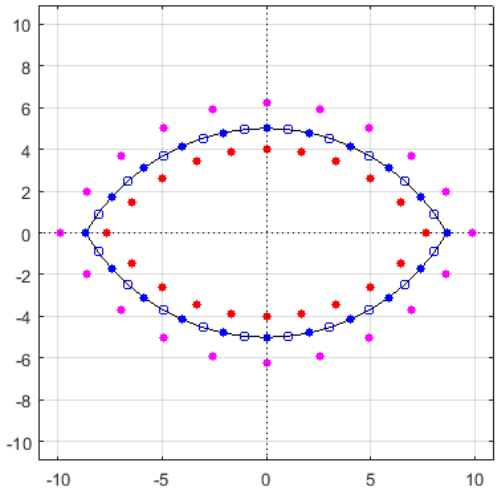

Fig. 1. a) Geometry of the scatterer (in blue) including inner auxiliary sources (AS's) (red) and outer auxiliary sources (AS's) (magenta). Blue dots stand for collocation points (CP's) and blue circles for midpoints (MP's).

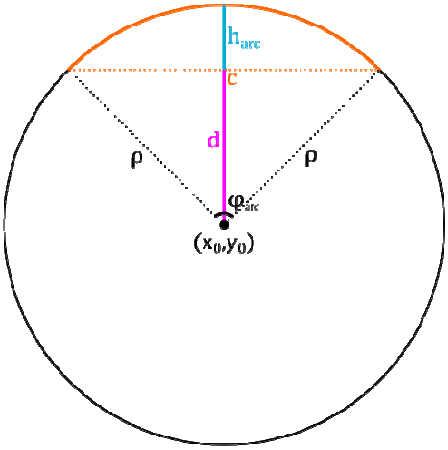

Fig. 1. b) Construction of the geometry.

3. IMPROVEMENT OF THE AUXILIARY SURFACE LAYOUT

As mentioned in [4],[5], MAS becomes less accurate when the auxiliary surfaces are conformal to boundaries including wedges. Specifically, satisfaction of the boundary condition at midpoints (MP's) (see Fig. 1a) close to the tips is no longer adequate. To overcome this complication, the auxiliary surface may be deformed so that AS's not only approach the tips closely, but become denser in the tip neighborhood as well. AS's may approach CP's following several patterns. In this work, two basic patterns were tested. Let M be the number of AS's to be moved. Let ρ_m be the polar radius of the m^{th} AS $(m = 1,2,\dots,M)$, let g be the maximum polar radius distance between the m^{th} AS and the m^{th} CP. Finally, let s be the proximity factor, defined in $[0,1]$, so that 0 corresponds to no approach and 1 corresponds to maximum approach (resulting in coincident AS's and CP's). Then, the schemes proposed for the auxiliary surface deformation are defined as follows:

$$\rho'_m = \rho_m + gs\left(\frac{m}{M}\right)^{\nu} \qquad (7)$$

where $\nu = 1$ for simple and $\nu = 2$ for progressive reach. The deformation effect is graphically described in Figs. 2,3.

Furthermore, as proposed in [5], AS's, and CP's accordingly, should become denser close to the wedge tip. Again, there is no unique way to accomplish this. In this work, the scheme implemented multiplies the polar angle φ_m of the m^{th} AS location by a factor D_m, $0 < D_{start} \le D_m \le 1$, where D_{start} is user-defined. For example, in the first quadrant of the 'eye', D_m is defined to be close to 0 for AS's near the wedge tip, and close to 1 for AS's close to the vertical axis. For progressive densification, the scheme proposed is: $\varphi'_m = \varphi_m D_m^2$. Moreover, additional AS's may be superimposed to the already existing ones close to the tips, if necessary (see Fig. 4)

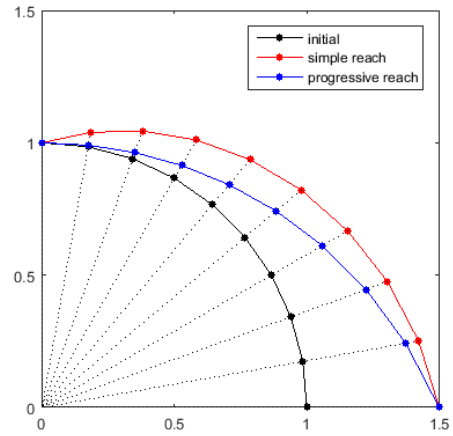

Fig. 2. Polar radius increase from 1 to 1.5 according to the proposed schemes

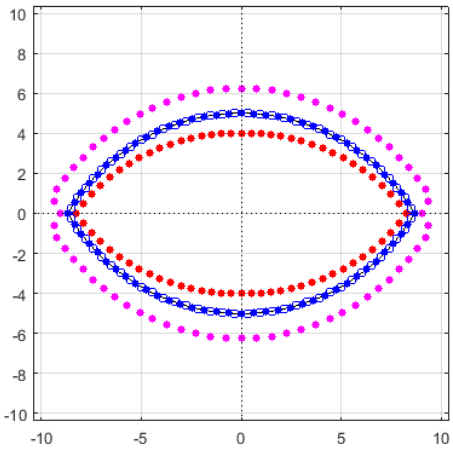

Fig. 3. Deformation of the auxiliary surface: all inner AS's are allowed to approach the CP's, whereas only 1/8 of the outer AS's are allowed to do so

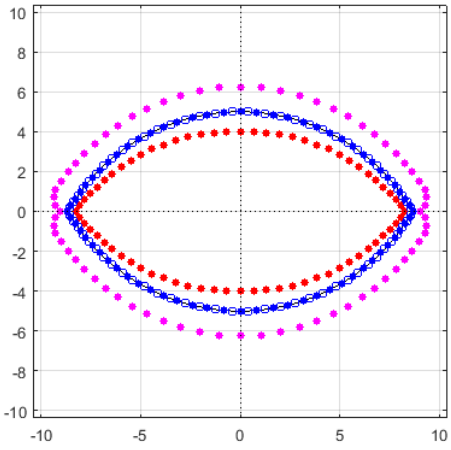

Fig. 4. Combination of tip approach and densification of the AS's

4. NUMERICAL RESULTS

To test the efficiency of the method, a scatterer is defined by radius $\rho = 3\lambda$, arc displacement $d = 1.5\lambda$, dielectric relative permittivity $\varepsilon_r = 2.56$, incidence angle $\varphi_{inc} = 0$, and originally $N = 160$ CP's, hence 160 inner and 160 outer AS's. Solution of the problem without any deformation yields the results of Fig. 5. The upper left subplot depicts the quantified error in the boundary condition (BC) of the E field along the boundary stretch, i.e.

$$\Delta E_{bc} = \frac{|\hat{\boldsymbol{n}} \times (\boldsymbol{E}_{in} - \boldsymbol{E}_{out})|}{E_0} \qquad (8)$$

where $\hat{\boldsymbol{n}}$ is the normal unit vector on the boundary, pointing outwards, and $\boldsymbol{E}_{in}, \boldsymbol{E}_{out}$ are the electric fields just inside and just outside the scatterer respectively. Similarly, the upper right subplot depicts the quantified error for the H field, and the lower plot illustrates the bistatic Radar Cross Section (RCS) in terms of the polar angle. It is obvious that the BC error is relatively significant in the immediate vicinity of the wedge tips.

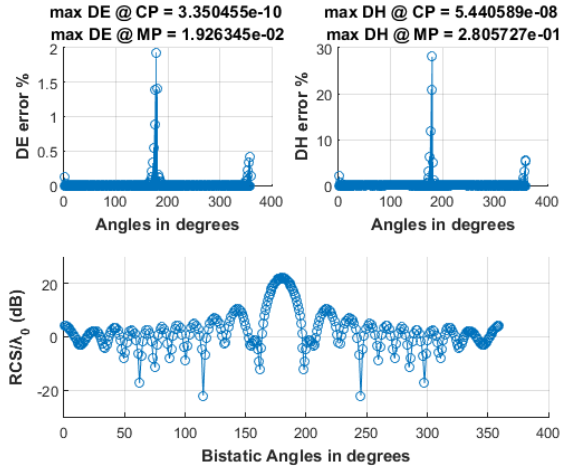

Fig. 5. Results for standard, conformal auxiliary surfaces

To improve satisfaction of the BC, the deformation scheme proposed above was implemented. After several trials, the following parameters were finally invoked: The portion of AS's to be displaced was $1/5$ for the inner and $1/8$ for the outer ones. The proximity factor was set equal to $s = 0.75$ for the inner and $s = 0.65$ for the outer AS's, while $D_{start} = 0.80$. No extra AS's were added, since their presence proved to be unimportant.

The results are shown in Fig. 6. The maximum E field error at MP's was reduced from $1.92 * 10^{-2}$ to $3.71 * 10^{-3}$ and the maximum H field error from $2.8 * 10^{-1}$ to $1.95 * 10^{-2}$. Although the RCS pattern is only slightly affected, more pronounced improvement is expected for larger scatterers.

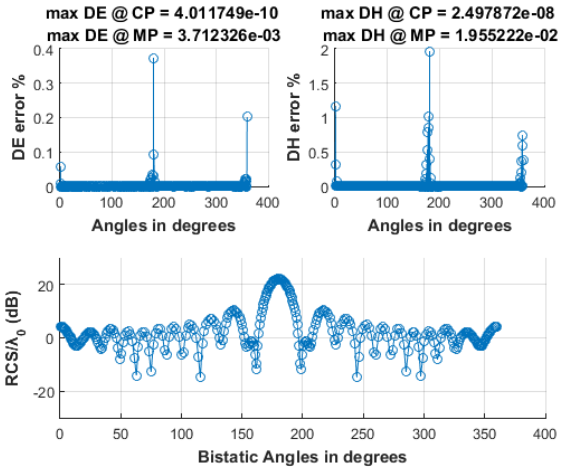

Fig. 6. Results for improved, non-conformal auxiliary surfaces

5. CONCLUSION

The Method of Auxiliary Sources (MAS) was applied to scattering from a dielectric cylinder with curved wedges. Since the BC error close to the wedge tips is significant for standard, conformal auxiliary surfaces, deformation of the latter was proposed. In the vicinity of the tips, both inner and outer AS's approached the CP's, and their distribution was also allowed to become denser. The BC error was proven to decrease significantly for both the E and the H field, yielding more accurate RCS results.

The authors wish to acknowledge financial support by the Special Account for Research Funds of the Technological Educational Institute of Central Macedonia, Greece, under grant SAT/IE /141/11/18-6-2014/80093.

References

[1] *R. S. Popovidi-Zaridze and Z. S. Tsverikmazashvili, "Numerical study of a diffraction problem by a modified method of non-orthogonal series", Zh vychisl. Mat. mat. Fiz., 17, 2, 1977, pp. 384-393.*

[2] *D. I. Kaklamani and H. T. Anastassiu, "Aspects of the Method of Auxiliary Sources (MAS) in Computational Electromagnetics", IEEE Antennas and Propagation Magazine, vol. 44, no. 3, June 2002, pp. 48-64.*

[3] *V. D. Kupradze, "On the approximate solution of problems of mathematical physics", Usp. mat. nauk, 22, no 2 (134), 1967, pp. 59-107.*

[4] *S. Eisler and Y. Leviatan, "Analysis of Electromagnetic Scattering from metallic and penetrable cylinders with edges using a Multifilament Current Model", IEE Proceedings, vol. 136, Pt. H, No. 6, Dec. 1989, pp. 431-438.*

[5] *H. T. Anastassiu, D. I. Kaklamani, D. P. Economou and O. Breinbjerg, "Electromagnetic Scattering Analysis of Coated Conductors with Edges Using the Method of Auxiliary Sources (MAS) in Conjunction with the Standard Impedance Boundary Condition (SIBC)", IEEE Trans. on Antennas and Propagation, vol. 50, no. 1, Jan. 2002, pp. 59-66.*

[6] *T. B. A. Senior and J. L. Volakis, Approximate Boundary Conditions in Electromagnetics, IEE Press, 1994.*